



# Evaluation of a new robotic spinal surgical system for K-wire placement characterized by tracker registration and lateral force sensing

Hailong Chen<sup>1</sup> · Yancheng Zhu<sup>1</sup> · Changzhi Du<sup>1</sup> · Yongkang Yang<sup>2</sup> · Jun Liu<sup>1</sup> · Liang Li<sup>2</sup> · Boyao Wang<sup>1</sup>

Received: 23 September 2025 / Accepted: 27 October 2025  
© The Author(s) 2025

## Abstract

**Background** Efficient registration and high-precision K-wire guidance are critical for the effective performance of spinal surgical robots. We therefore evaluate a new robotic system featuring optical tracker registration and a high-precision lateral force sensing system during K-wire placement. In this study, retrospectively collected clinical data were used to evaluate the technical efficacy and clinical utility of the system in spinal surgery.

**Methods** This was a retrospective study. Between December 2022 and April 2024, a total of 127 patients were enrolled and subjected to X-ray, CT, and MRI examinations. Among these patients, 67 were enrolled in the robot-assisted group, in which K-wires were implanted using a new spinal surgical robot. The remaining 60 patients were enrolled in the freehand group, where K-wires were implanted manually. The data collected included sex, age, body mass index, number of punctures (NOP), mean time required to insert a K-wire (MTRI K-wire), average blood loss per K-wire insertion (ABL K-wire), fluoroscopy count per K-wire (FC K-wire), puncture abduction angle (PAA), and K-wire in the pedicle (K-wire IP). Distance deviations and angle deviations were used as the primary parameters to evaluate the accuracy of the new spinal surgical robot.

**Results** Compared with free-hand K-wire insertion, robot-assisted K-wire implantation results in fewer NOP, fewer MTRI K-wires, fewer ABL K-wires, fewer intraoperative FC K-wires, and a larger PAA. Compared with the free-hand group, the robot-assisted group demonstrated significantly smaller entry point deviation ( $0.98 \pm 0.13$  vs.  $5.08 \pm 1.17$  mm,  $p < 0.001$ ) and endpoint deviation ( $1.38 \pm 0.20$  vs.  $5.52 \pm 0.87$  mm,  $p < 0.001$ ). These results demonstrate superior targeting accuracy with robotic assistance relative to conventional freehand techniques.

**Conclusions** Our spinal surgical robot system demonstrates clinically reliable accuracy in K-wire placement while offering significant intraoperative advantages, including a streamlined procedural workflow, a reduced operation time, and minimal tissue trauma. These results demonstrate significant potential for both clinical implementation and further technological optimization.

**Trial registration** This trial was approved by the Ethics Committee of the Second Affiliated Hospital of Nanjing Medical University on February 21, 2023(2023XJ00401 retrospectively registered).

**Keywords** Robot-Assisted spinal surgery · Accuracy · K-Wire · Tracker registration · Lateral force sensing

Hailong Chen and Yancheng Zhu contributed equally to this manuscript.

✉ Jun Liu  
13776698080@139.com

✉ Liang Li  
liliang@njmu.edu.cn

✉ Boyao Wang  
13912980806@163.com

<sup>1</sup> Department of Spine Surgery, The Second Affiliated Hospital of Nanjing Medical University, Nanjing 210003, China

<sup>2</sup> Nanjing Medical University, Nanjing 210003, China

## Abbreviations

K-wire	Kirschner wire
X-ray	X-radiation
CT	Computed tomography
MRI	Magnetic Resonance Imaging
NOP	Number of punctures
MTRI K-wire	Mean time required to insert a K-wire
ABL K-wire	Average blood loss per K-wire insertion
FC K-wire	Fluoroscopy count per K-wire
PAA	Puncture abduction angle
K-wire IP	K-wire in the pedicle
3D	Three-dimensional
SVD	Singular value decomposition
ICP	Iterative closest point
mm	Millimeter
N/A	Not Available

## Background

In spinal surgery, robotic systems enhance surgical precision by providing advanced intraoperative imaging and accurate instrument guidance [1]. Following the acquisition of three-dimensional (3D) imaging data, the robotic system reconstructs a patient-specific spinal model, facilitating the preoperative planning of optimal pedicle screw trajectories. The platform subsequently offers real-time intraoperative navigation, ensuring precise execution of the planned surgical procedure with submillimeter accuracy. Extensive clinical evidence confirms that robot-assisted lumbar pedicle screw fixation demonstrates significantly greater placement accuracy compared to conventional free-hand techniques [2–4]. Emerging evidence supports the efficacy of robotic-assisted spinal systems in complex procedures, including interbody fusion, spinal tumor resection, vertebroplasty, and deformity correction osteotomies [5, 6].

The initial development of robotic spinal surgery systems commenced in the 1990s; however, technical limitations—including software instability, suboptimal image-to-robot registration accuracy, restricted robotic arm maneuverability, and nonintuitive user interfaces—have impeded their clinical integration and widespread adoption [7, 8]. The Mazor SpineAssist system emerged as the first clinically validated robotic system for spinal surgery, maintaining exclusive FDA approval for robotic-assisted spinal procedures from 2004 to 2011. The system employed a patient-mounted tracking platform and integrated preoperative computed tomography (CT) data with intraoperative fluoroscopic imaging to facilitate the precise planning of pedicle screw trajectories [9]. In addition, technological evolution has driven the rapid development of various robotic-assisted spinal surgery systems, such as Renaissance, Mazor

X (Medtronic), ROSA (Medtech®), ExcelsiusGPS (Globus Medical), MAXIO (Globus Medical), TianJi, Cirq (Brainlab), Curexo (CUREXO, Inc.), Kinguide (Point Robotics), and Remi (Accelus) [10]. Most spinal surgical robotic systems are classified as semiactive, collaborative platforms that enhance operative precision, procedural efficiency, and intraoperative stability through real-time navigational guidance while preserving the surgeon's autonomous control over critical technical execution and clinical decision-making throughout the operative process [11].

Despite advancements, contemporary surgical robots still face significant limitations. Most systems rely on marker-based registration, which necessitates the placement of fiducial markers near the patient. This requirement complicates the registration process and prolongs the operative time. Second, real-time monitoring of K-wire insertion is currently unfeasible. This limitation poses a particular challenge during thoracic vertebral procedures, where respiration-induced motion can lead to significant deviations in K-wire placement.

To address these challenges, our team previously developed a new spinal surgical robot. This system incorporates an optical tracker integrated with a 3D C-arm and features a high-precision lateral force sensing system within the robotic end effector. The new surgical robot employed in this study incorporates two primary innovations. During the registration process, an intraoperative integrated adaptive registration technique based on C-arm trajectory recognition and calibration was employed. This approach requires only the acquisition of the C-arm spatial motion trajectory, through which the entire registration procedure is completed by leveraging trajectory recognition algorithms combined with singular value decomposition (SVD) and iterative closest point (ICP) algorithms. This methodology optimizes the registration workflow while enhancing both registration accuracy and real-time efficiency. In addition, the K-wire insertion process is equipped with a unique real-time tip force sensing capability, which effectively mitigates intraoperative skidding on bone surfaces and minimizes soft tissue injury.

The new robotic system has been deployed in 127 consecutive percutaneous vertebroplasties and robot-assisted pedicle screw fixations at our institution since December 2022. This retrospective study aims to analyze collected clinical and radiological data, with the primary objectives of quantifying K-wire placement accuracy based on distance and angle deviations and evaluating clinical outcomes.

## Methods

### Robotic surgical system

#### Core components

The new spinal surgical robot system consists of a three-dimensional imaging C-arm X-ray machine, an optical tracking system cart, and a surgical navigation and positioning robot (Fig. 1). It integrates intraoperative three-dimensional imaging, navigation positioning, and surgical planning functionalities. The spinal surgical robot system employed in this study, named the Perlove Spinal Surgical Robot, was collaboratively developed by our research team and Perlove Medical.

#### Optical tracker registration method

Figure 2 shows the optical tracker for the 3D C-arm. This study employed a new automatic registration method integrated into the spinal surgical robot system. The method relies on an optical tracker rigidly mounted on the detector of the 3D C-arm. During intraoperative 3D imaging, the navigation system tracks the C-arm's position and orientation in real-time. Immediately following image acquisition, the reconstructed 3D dataset and its spatial coordinates are automatically transmitted to the robot, thereby achieving

instantaneous registration between the image space and the robotic surgical space.

#### High-precision lateral force sensing system method

Figure 3 shows the high-precision lateral force sensing system integrated into the robotic end effector. During the surgeon's K-wire implantation procedure, the optical tracking system cart screen displays real-time deviations between the actual K-wire insertion path and the preoperatively planned path. The "skiving" phenomenon, where a K-wire slides along a non-perpendicular or irregular cortical surface, is a primary cause of trajectory deviation during surgical insertion. This issue is magnified in percutaneous spine procedures due to lateral forces from soft tissue tension and the often-inclined surfaces of pedicle entry points. Conventional methods and standard robotic systems lack the ability to perceive these subtle mechanical disturbances, leading to repeated attempts, prolonged procedures, and an increased risk of iatrogenic injury to critical structures like nerve roots. To address this, our system incorporates a high-precision 3D lateral force sensor within the end-effector. This module monitors real-time shear forces and moments on the K-wire, synchronizing this data with the navigation software. When anomalous lateral forces indicative of skiving is detected, the system generates color-coded visual alerts and displays quantitative deviations (entry, tip, and angular errors) on the navigation screen. This actionable

**Fig. 1** The components of the new spinal surgical robot system comprise a three-dimensional imaging C-arm X-ray machine, an optical tracking system cart, and a surgical navigation and positioning robot

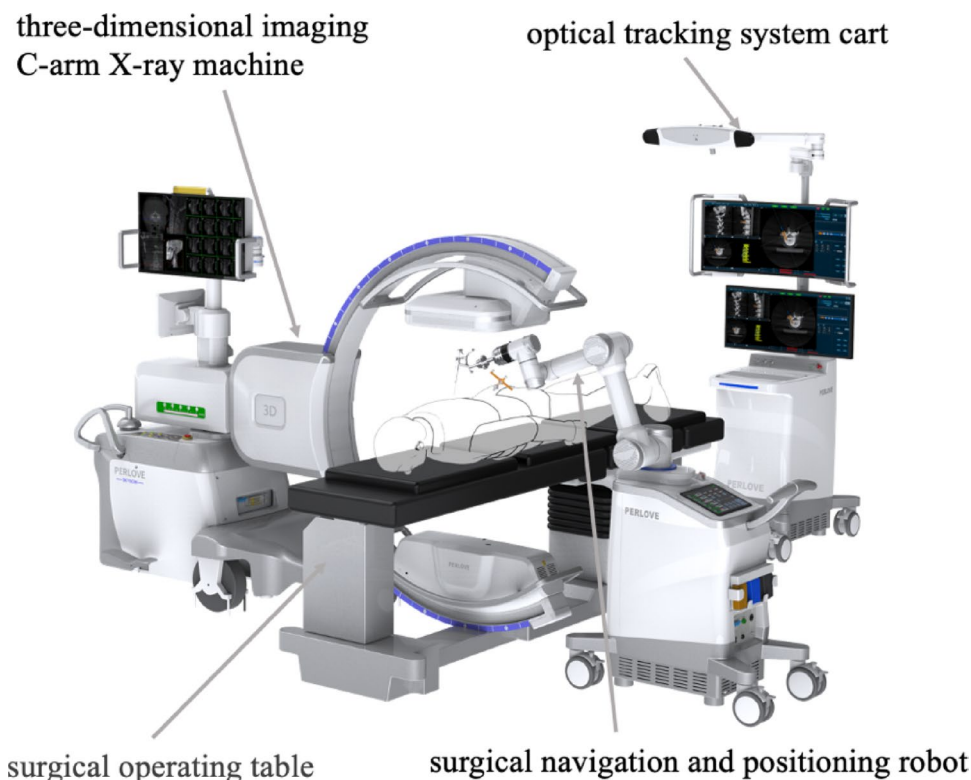




**Fig. 2** Integration of the optical tracker with the 3D C-arm. (A) An optical tracker is rigidly mounted on the detector of the 3D C-arm, shown here in its pre-planned initial scanning position. (B–D) During 3D image acquisition, the C-arm rotates continuously along a predefined arcuate trajectory (indicated by the red arrow). This motion trajectory is captured in real-time by the optical navigation system and serves as the foundational input for the subsequent trajectory-based, markerless spatial registration algorithm

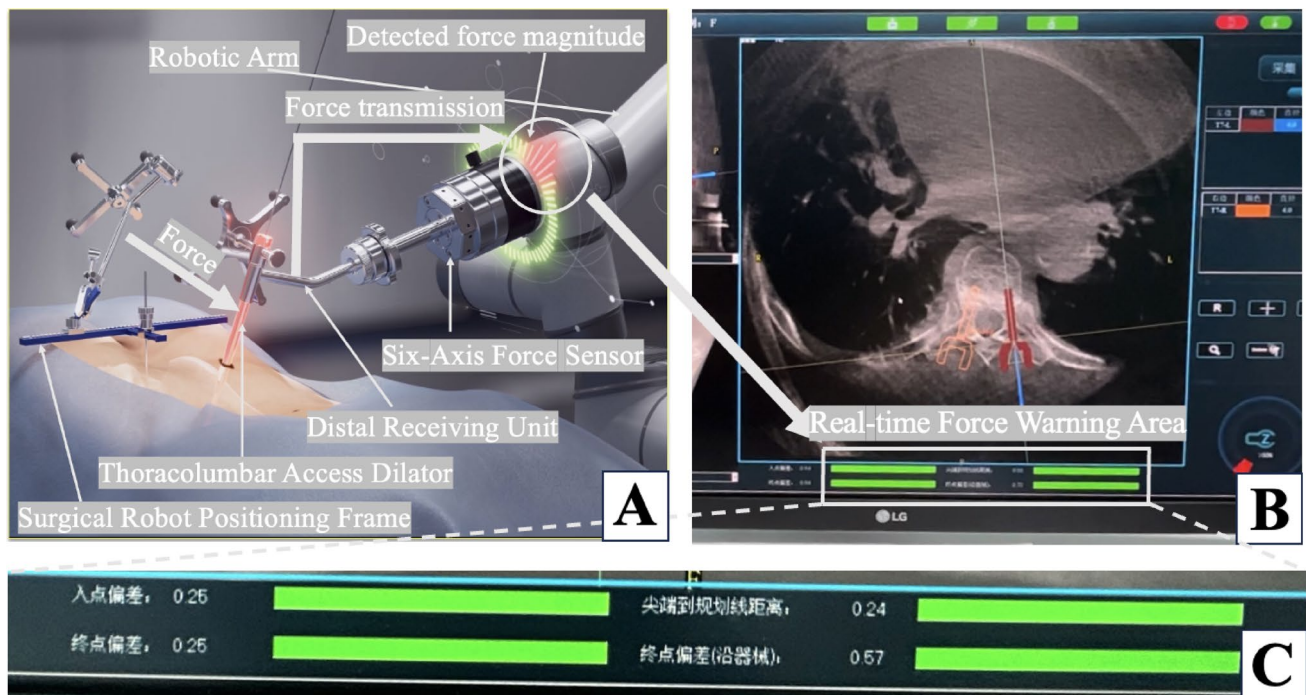
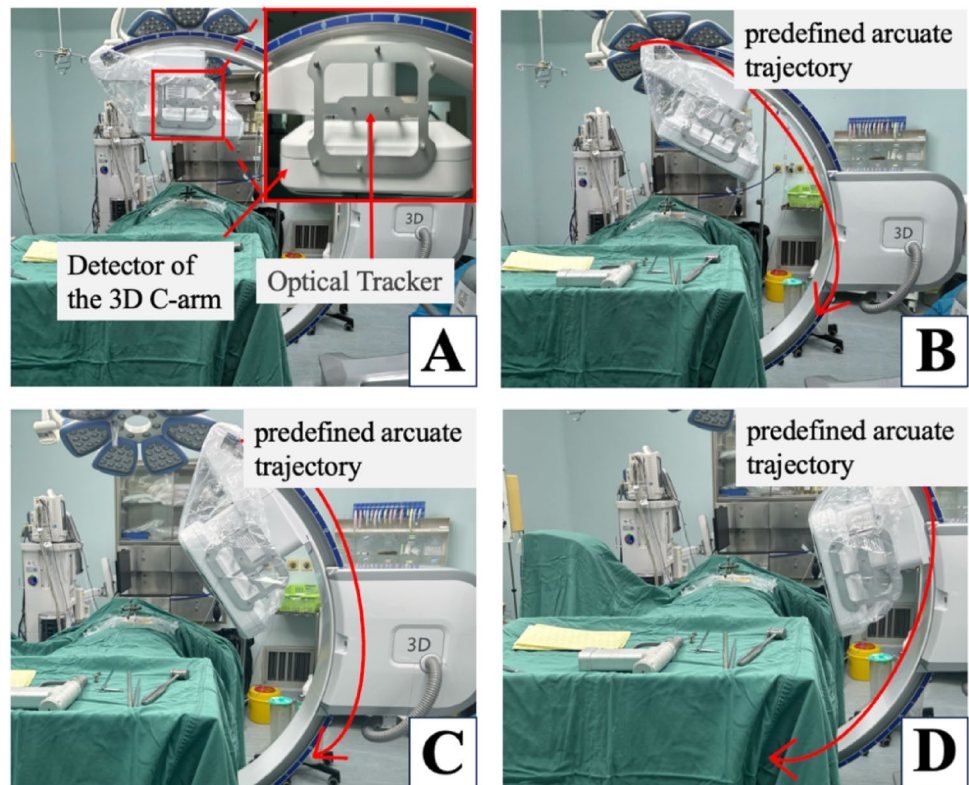


**Fig. 3** High-precision lateral force sensing system and its navigation interface feedback. (A) The robotic end-effector is equipped with a six-axis force/torque sensor for real-time detection of forces on the K-wire during insertion. (B) The navigation software integrates force data with spatial tracking to visualize deviations between the actual

and planned trajectories. (C) Display key accuracy metrics: entry point deviation (0.25 mm), tip-to-trajectory distance (0.24 mm), end point deviation (0.25 mm), and end point deviation along the instrument axis (0.57 mm)

feedback enables the surgeon to make immediate corrective adjustments, thus preventing trajectory deviation and ensuring accurate K-wire placement.

### Surgical workflow of the new robotic surgical system

The key procedural workflow for robot-assisted K-wire placement in the new spinal surgical system comprises the following stages: (1) Image Acquisition Phase, (2) Image Processing and Registration Phase, (3) Surgical Planning Phase, (4) Robotic Positioning Phase, (5) Surgical Execution Phase, and (6) Verification Phase (Fig. 4).

### Preoperative planning

Prior to the surgical procedure, the navigation system was initialized by activating the device power supply and launching the operational software. Patient demographic data were registered, followed by the selection of three-dimensional image orientation parameters aligned with the patient's decubitus position and C-arm configuration. Upon completion of 3D C-arm registration, patient data were synchronized to the optical tracking system cart. The navigation interface was subsequently initialized using optical tracking software. Three-dimensional image acquisition was then performed, with volumetric datasets automatically transferred from the C-arm workstation to the tracking cart for intraoperative navigation access.

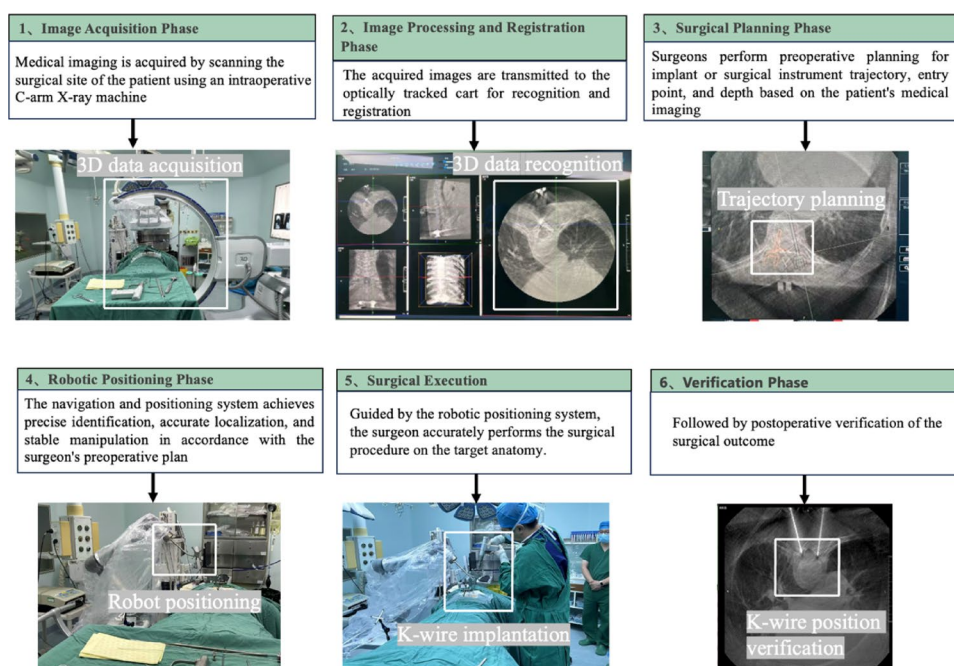
### Intra-operative robot registration

Following preoperative planning, the optical tracking system was deployed for trajectory planning of the K-wire. The optimal entry points and insertion depths were computationally determined using integrated planning software. The robotic manipulator cart was then positioned adjacent to the operative table. Spatial registration was achieved by acquiring the manipulator's base tracer coordinates. Subsequent fiducial registration incorporated the robotic coordinates into the navigation space. Upon validation of targeting accuracy, the robotic arm executed autonomous positioning to preplanned coordinates, with final trajectory confirmation against intraoperative CT benchmarks.

### Surgery implementation

Following robotic positioning, a percutaneous stab incision was created along the planned trajectory using a trocar-tipped lancet. Through this access, a cannulated sleeve was deployed to the lamina surface. The K-wire was advanced into the vertebral body via a powered drill through the guiding sleeve. This procedure was iteratively performed for all predetermined trajectories. Upon completion, the robotic platform was retracted from the surgical field. Postimplantation verification was conducted using intraoperative 3D imaging with multiplanar reconstruction to assess the accuracy of K-wire placement.

**Fig. 4** The key procedural workflow for robot-assisted K-wire placement using the new spinal surgical system



## Clinical data acquisition

Age, sex, BMI, Bone mineral density, average number of k-wires, and number of surgical segments were recorded. The number of punctures (NOP) is defined as the total number of percutaneous insertion attempts required to achieve successful implantation of a K-wire. The mean time required to insert a K-wire (MTRI K-wire) is defined as the average duration required for successful percutaneous implantation of a K-wire, measured from initial skin penetration to final radiographic confirmation of position. The average blood loss per K-wire insertion (ABL K-wire) is defined as the average volume of hemorrhage occurring during successful percutaneous implantation of a K-wire, quantified from initial skin penetration until final fixation. The fluoroscopy count per K-wire (FC K-wire) is defined as the number of radiographic exposures required to achieve successful percutaneous implantation of a K-wire. The puncture abduction angle (PAA) is defined as the angle between the K-wire trajectory and the midline of the vertebral body. The K-wire in the pedicle (K-wire IP) is defined as complete intraosseous positioning of the K-wire within both the pedicle and vertebral body boundaries, verified on postoperative CT reconstructions with no cortical breach observed in any plane.

## K-wire accuracy assessment

### A clear methodology for determining the entry and end point deviations

The overall flowchart of the deviation calculation method is shown in Fig. 5. First, the deviation calculation method uses a preprocessing method, including image threshold

segmentation and morphology, to segment the lumbar vertebrae in the three-dimensional C-arm CT planning image and postoperative C-arm CT image. The segmented lumbar vertebrae are then converted into point cloud form. Afterward, the iterative closest point registration method is used to achieve three-dimensional registration of the point cloud of the lumbar vertebra from the planning image and the postoperative image, resulting in the calculation of the registration deformation matrix. Then, this registration deformation matrix is then applied to the planned paths for pedicle screws to map it from the planning image space to the postoperative image space. The K-wires in postoperative C-arm CT images are segmented using the above preprocessing method. Finally, deviations in the entry points, end points, and angles of insertion between the mapped planned path and the actual implanted K-wires can be calculated in the same postoperative image space.

### Detailed calculations or formulas used to quantify these deviations

The  $i$ -th implanted K-wire and the corresponding planned path are shown in Fig. 6, where the planned path has been mapped from the planning image space to the postoperative image space. The entry and end points of the  $i$ -th implanted K-wire are  $p_{i,1}$  and  $p_{i,2}$ , respectively, whereas the entry and end points of the corresponding planned path are  $p'_{i,1}$  and  $p'_{i,2}$ , respectively. These formulas calculate a simple Euclidean distance between the two points.

The distance deviation  $d_1$  for the entry point between the  $i$ -th implanted K-wire and the corresponding planned path can be calculated using Formula (1) [12] as follows:

**Fig. 5** Overall flowchart of the deviation calculation method

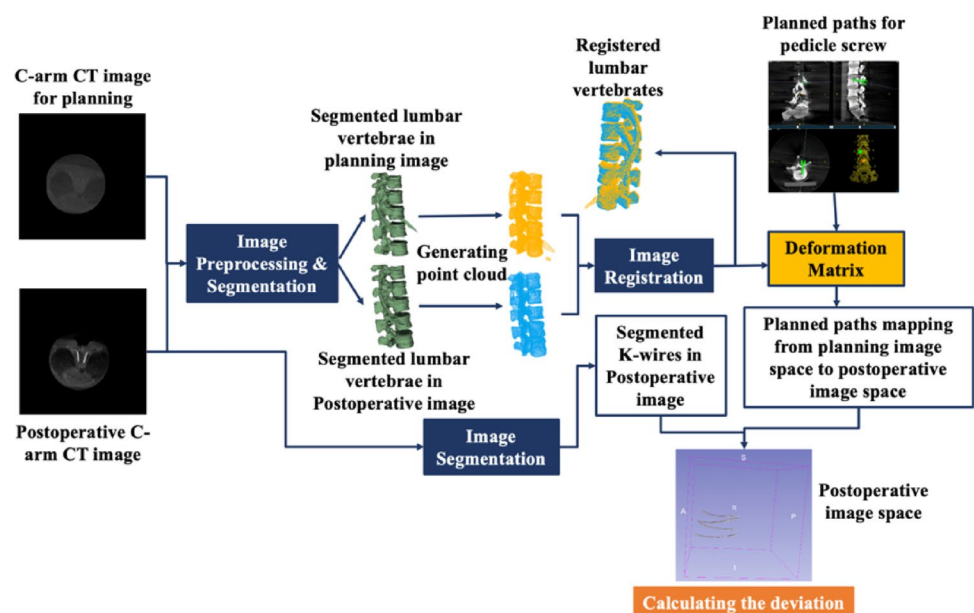
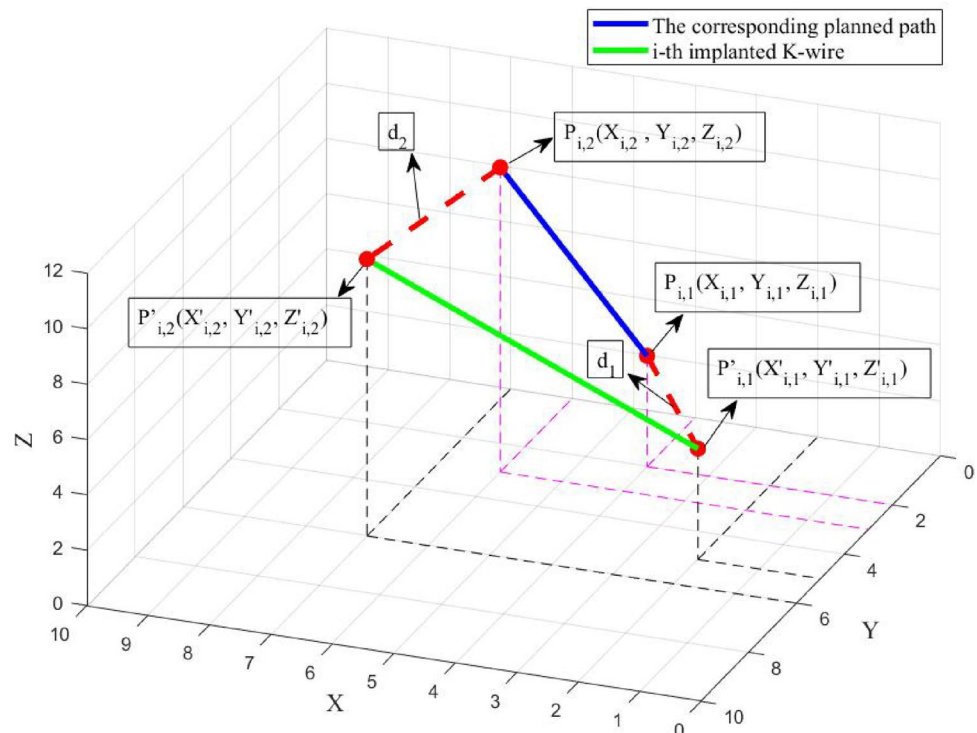




**Fig. 6** Illustration of the  $i$ -th implanted K-wire and the corresponding planned path in the postoperative image space. The red line denotes the implanted K-wire, and the green line denotes the corresponding planned path



$$d_1 = \sqrt{(x_{i,1} - x'_{i,1})^2 + (y_{i,1} - y'_{i,1})^2 + (z_{i,1} - z'_{i,1})^2} \quad (1)$$

Similarly, the distance deviation  $d_2$  for the endpoint between the  $i$ -th implanted K-wire and the corresponding planned path can be calculated using Formula (2) [13] as follows:

$$d_2 = \sqrt{(x_{i,2} - x'_{i,2})^2 + (y_{i,2} - y'_{i,2})^2 + (z_{i,2} - z'_{i,2})^2} \quad (2)$$

The angle deviation  $\alpha$  between the  $i$ -th implanted K-wire and the corresponding planned path can be calculated using Formula (3) [14] as follows:

$$\alpha = \cos^{-1} \frac{p_{i,1} \bar{p}_{i,2} \cdot p'_{i,1} \bar{p}'_{i,2}}{|p_{i,1} \bar{p}_{i,2}| \cdot |p'_{i,1} \bar{p}'_{i,2}|} \quad (3)$$

## Research design

This study is a retrospective study and was approved by the Ethics Committee. From December 2022 to April 2024, 127 patients who met the inclusion and exclusion criteria were implanted with K-wires using freehand fluoroscopy assistance or new spinal surgical robot assistance. All patients were fully aware of the possible risks of the operation and signed informed consent before the operation. All operations were performed by a senior deputy chief physician of

spinal surgery at the Second Affiliated Hospital of Nanjing Medical University from December 2022 to April 2024. For the robot-assisted surgery group, a three-dimensional C-arm machine was used in conjunction with a new spinal surgical robot to obtain the patient's anterior and lateral views and 3D images of the spine. The inclusion criteria were as follows: (1) Suitable for general anesthesia, with an American Society of Anesthesiologists (ASA) physical status classification of I, II, or III; (2) Diagnosed with vertebral compression fracture, spinal canal stenosis, or lumbar scoliosis requiring surgical intervention, as confirmed by radiological findings; (3) Provided written informed consent from the patient and/or their legal guardian to undergo robot-assisted percutaneous vertebroplasty (PVP) or percutaneous pedicle screw fixation (PPSF). The exclusion criteria were: (1) Severe or complex spinal deformities (e.g., Cobb angle  $>40^\circ$  or deformities requiring osteotomy); (2) Presence of spinal tumors, infections, or active tuberculosis; (3) History of previous surgery at the target spinal segments; (4) Spondylolisthesis of Meyerding grade II or higher; (5) Uncorrected coagulopathy or ongoing anticoagulation therapy; (6) Pregnancy or lactation; (7) Presence of severe, uncontrolled systemic diseases (e.g., severe cardiac, pulmonary, hepatic, or renal insufficiency). The participants retained the right to withdraw from the trial at any point without penalty. The study will be immediately discontinued per protocol-specified stopping rules upon the occurrence of serious adverse events.

**Table 1** Baseline characteristics of patients

	Free-hand group	Robot-assisted group	<i>P</i> value
Age	60.06±7.52	59.79±6.39	0.825
Female ratio	55.0%	67.2%	0.160
BMI	25.80±1.98	26.46±2.05	0.070
BMD	-1.56±0.80	-1.69±0.83	0.337
Average number of k-wire	2.80±1.34	2.84±1.36	0.881
Surgical segments			
T11	4	5	
T12	21	29	
L1	29	36	
L2	14	13	
L3	9	8	
L4	5	3	
L5	2	1	

BMI body mass index, BMD Bone Mineral Density

**Table 2** Radiological measurements and clinical results of K-wire placement

	Free-hand group	Robot-assisted group	<i>P</i> value
NOP	9.85±3.18	1.11±0.35	<0.001
MTRI K-wire	18.42±6.03	11.84±2.31	<0.001
ABL K-wire	15.72±2.67	7.11±1.49	<0.001
FC K-wire	7.46±1.64	2.48±1.13	<0.001
PAA	10.05±3.58°	23.66±2.45°	<0.001
K-wire IP	142/168 (84.5%)	183/190 (96.3%)	<0.001

## Statistical analysis

Independent samples *t* tests and chi-square tests were employed to compare the baseline characteristics, imaging parameters, and clinical outcomes between the two cohorts. All of the statistical analyses and graph plotting were performed using SPSS 27.0 and Origin 2024. Statistical significance was defined as  $P < 0.05$ .

## Results

### Baseline characteristics and distribution of surgical segments

A total of 127 patients were recruited and enrolled in the study between December 2022 and April 2024. The freehand group comprised 60 patients, with a total of 168 K-wires implanted. In contrast, the robot-assisted group comprised 67 patients, with a total of 190 K-wires implanted. No statistically significant differences were observed between the baseline characteristics of the patients (Table 1).

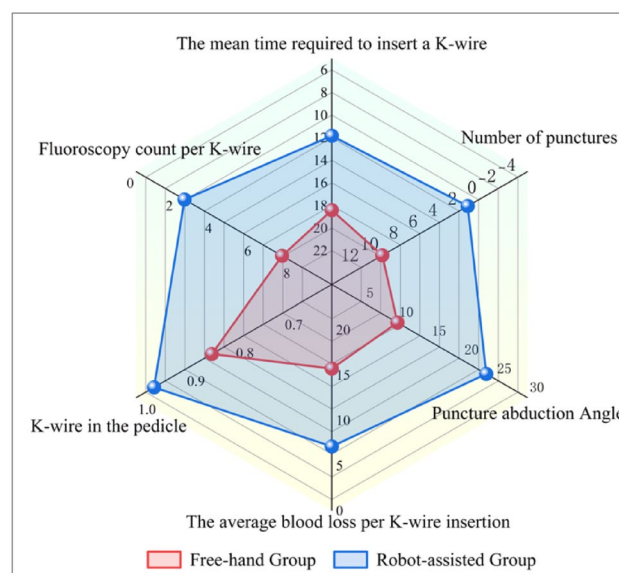


**Fig. 7** Radar chart comparing the radiological measurements and clinical results of K-wire placement in the freehand group and robot-assisted group. All comparisons were statistically significant ( $P < 0.001$ )

### Clinical and radiographic assessment of K-wire placement

The data and analyses of the number of punctures (NOP), the mean time required to insert a K-wire (MTRI k-wire), the average blood loss per K-wire insertion (ABL K-wire), the fluoroscopy count per K-wire (FC K-wire), the puncture abduction angle (PAA), and the K-wire in the pedicle (K-wire IP) are included in Tables 2 and Fig. 7. The robot-assisted group demonstrated statistically superior outcomes across all parameters ( $P < 0.001$ ), including significantly fewer punctures ( $1.11 \pm 0.35$  vs.  $9.85 \pm 3.18$ ), shorter K-wire insertion times ( $11.84 \pm 2.31$  vs.  $18.42 \pm 6.03$  minutes), decreased blood loss per insertion ( $7.11 \pm 1.49$  vs.  $15.72 \pm 2.67$  ml), and lower fluoroscopy counts per K-wire ( $2.48 \pm 1.13$  vs.  $7.46 \pm 1.64$ ), while achieving greater trajectory abduction angles ( $23.66 \pm 2.45^\circ$  vs.  $10.05 \pm 3.58^\circ$ ). Crucially, robotic assistance demonstrated significantly superior interpedicular accuracy ( $183/190$  [96.3%] vs.  $142/168$  [84.5%]), a K-wire placement was defined as ‘interpedicular’ if its entire trajectory was contained within the pedicle, showing no evidence of cortical violation.

### Radiographic measurement of K-wire insertion deviations

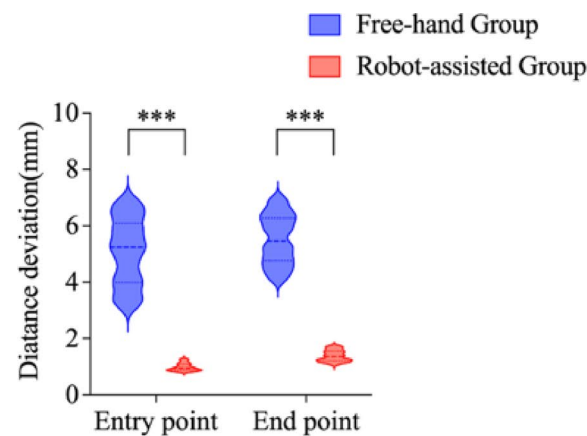
The insertion deviation of the K-wire was evaluated based on three key metrics: entry point deviation (Formula 1), endpoint deviation (Formula 2), and angular deviation (Formula 3). The results, which are consistent with the data presented in Table 3, are visually illustrated in Fig. 8. Robotic



**Table 3** Comparison of preoperative and postoperative results between the freehand group and the robot-assisted group

		Free-hand group	Robot-assisted group	P value
3D distance	Entry point deviation	(5.08±1.17) mm	(0.98±0.13) mm	<0.001
	End point deviation	(5.52±0.87) mm	(1.38±0.20) mm	<0.001
Angle deviation	ZOY plane	8.01±1.11°	0.98±0.21°	<0.001
	ZOX plane	10.49±1.35°	1.43±0.25°	<0.001
	XOY plane	10.98±1.75°	0.96±0.10°	<0.001

assistance significantly reduced 3D deviations compared with the freehand technique, with entry point deviations (0.98±0.13 mm vs. 5.08±1.17 mm;  $P<0.001$ ) and end point deviations (1.38±0.20 mm vs. 5.52±0.87 mm;  $P<0.001$ ) demonstrating superior spatial targeting accuracy. Robotic assistance significantly reduced K-wire angular deviations compared with freehand assistance across all cardinal planes (all  $P<0.001$ ), achieving subdegree precision in the ZOY plane (0.98±0.21° vs. 8.01±1.11°), ZOX plane (1.43±0.25° vs. 10.49±1.35°), and XOY plane (0.96±0.10° vs. 10.98±1.75°) (Table 3; Fig. 8).

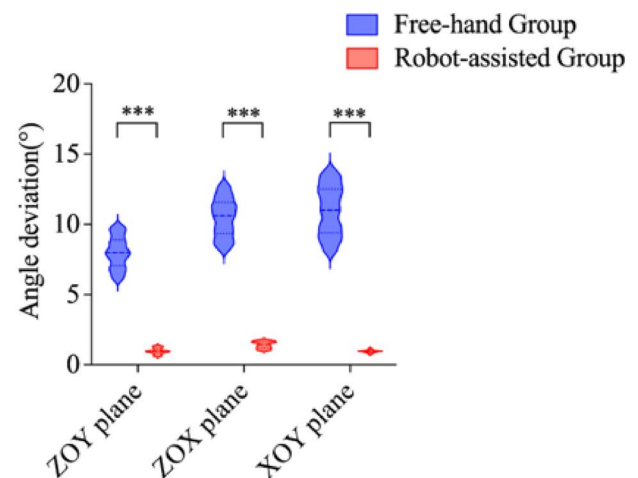


## Comparison of deviations with previous studies

A comparison of these deviations with previous studies highlights the improvements offered by this new spinal surgical robot (Table 4).

## Discussion

The accuracy of pedicle screw placement remains a critical determinant of clinical outcomes in spinal surgery. While robotic systems have been developed to mitigate the challenges of freehand techniques, their reported accuracy varies in the literature. Our study contributes to this field by demonstrating an overall accuracy of 96.3% for robot-assisted K-wire insertion, with all misplacements considered clinically acceptable. This level of precision is consistent with several prior investigations, which have documented accuracy rates between 85% and 100% for robot-guided screws [15–19]. For example, Keric et al. [18] and Kantelhardt et al. [15] reported similar high success rates of 96.9% and 94.5%, respectively. While our results reinforce the reliability of

**Fig. 8** Violin plot showing that the free-hand group has significantly greater distance deviation and angle deviation compared with the robot-assisted group**Table 4** A comparison with previous studies

	Tuoshou [12]	TiRobot [12]	ROSA [13]	Excelsius GPS [14]	Prelove
Average deviation (mm)	1.66 (1.14–2.31)	1.89 (1.18–2.62)	N/A	N/A	N/A
Entry point deviation (mm)	1.55 (0.93–2.09)	1.88 (1.20–3.12)	2.05±1.2	2.1 (0.8–5.2)	0.98 (0.78–1.30)
End point deviation (mm)	1.77 (1.22–2.60)	1.70 (1.07–2.40)	1.57±1.01	3.2 (0.9–5.4)	1.38 (1.02–1.75)
Average angle deviation (°)	Axial: 0.72 (0.26–1.35) Sagittal: 0.99 (0.51–1.84) Spatial: 1.55 (0.91–2.43)	Axial: 0.69 (0.16–1.67) Sagittal: 1.18 (0.54–2.02) Spatial: 1.57 (0.93–2.70)	N/A	2.4 (0.7–3.8)	ZOY: 0.98 (0.59–1.39) ZOX: 1.43 (1.00–1.79) XOY: 0.96 (0.70–1.21)

Note: Data are reported in their original format from the source literature: Tuoshou and TiRobot as median (IQR); ROSA as mean±SD; and ExcelsiusGPS and Prelove as mean (range, min–max)

this technology, it is important to note the conflicting report from Ringel et al. [19], who found manual techniques to be superior. Such variability across studies, alongside our own findings, underscores that performance is likely influenced by the specific robotic system used, the surgical learning curve, and the patient population [20, 21]. Therefore, our findings provide further validation for the Prelove platform in achieving safe and accurate K-wire placement.

Although studies have demonstrated that robotic assistance can improve the accuracy of screw placement in spinal surgery, intraoperative complications may persist, and novel complications may arise. As this technology is relatively new, we currently lack a comprehensive understanding of the potential sources of K-wire insertion errors and associated complications. It is imperative to minimize these errors by refining both the robotic technology and the surgical workflow on the basis of a thorough understanding of their underlying causes. As noted above, Gautam et al. [22] classified errors into three categories: registration errors, skiving errors, and interference errors. Registration errors occur when the imaging software fails to detect osseous surface anatomical landmarks accurately due to poor bone quality, the presence of prior implants, severe deformity, or suboptimal imaging quality. These errors are also associated with the precision of the matching algorithm during spatial registration and the accuracy of the positioning camera. Furthermore, loose mounting of the tracker within the skeletal anatomy in robotic systems may lead to unintended intraoperative movement, resulting in registration drift. Consequently, successful registration in robotic applications is critically dependent on achieving tight, rigid, and secure tracker attachment to the spine. In the present study, the tracker was affixed to the spinous process of the inferior vertebra using a thick K-wire, with additional stabilization provided by a sterile drape to prevent registration drift. Skiving errors, a frequent complication during spinal instrumentation procedures, refer to the phenomenon of tool slippage on the cortical surface at the planned entry point [23]. These inaccuracies arise when the preoperatively planned entry point is situated on an irregular, sclerotic, or steeply inclined vertebral surface, causing the K-wire to skive. Furthermore, during percutaneous approaches, inadequate soft tissue dissection can lead to fascial and muscular tension exerting force on the K-wire, resulting in errors. Additionally, the use of low-speed drills may cause the K-wire to bind against the cannula axis, altering its trajectory and inducing skiving upon contact with the osseous surface. The accurate engagement of a guide wire or screw at the predetermined entry point is fundamental to successful pedicle screw fixation. A significant impediment to this initial step is the phenomenon of tool skiving, where the instrument slips on the cortical surface, leading to trajectory deviation and eventual

screw malposition. The prevalence and clinical significance of skiving are well-documented in the literature. Hu et al. [24] reported that tool skiving was responsible for all 1.1% of the screw placement errors observed in their cohort. Furthermore, a systematic review by Gautam et al. [22] found that skiving contributed to 26.8% of all reported inaccuracies. It is noteworthy that this problem persists even with the adoption of advanced robotic systems, as one study documented that skiving was the cause of 69% (22/32) of screw misplacements [25]. The sequelae of skiving can be severe. Beyond the immediate risk of iatrogenic injury to neural or vascular structures, which can result in catastrophic complications, the resultant suboptimal screw placement may also compromise the mechanical integrity of the fixation, predisposing the construct to failure. Therefore, the mitigation of skiving errors is not only pivotal for improving surgical precision and patient safety but also remains a key challenge for the development of next-generation surgical navigation systems and instrumentation. To mitigate these risks in percutaneous procedures, we recommend the following: (1) utilizing cannulas with serrated tips at the distal end to enhance osseous anchorage; (2) creating a small pilot hole at the intended entry site when employing steeply angled trajectories to prevent skiving; (3) avoiding steep bony surfaces prone to deflection during K-wire entry point selection in surgical planning; and (4) preferentially employing high-speed drills for K-wire insertion. Interference errors arise from unintended interactions among surgical instruments, the robotic system, patient anatomy, and the surgical field. One notable example of such interference in robotic spinal surgery involves pressure exerted by soft tissues on the guidance robotic arm.

Conventionally, spinal surgical robots have widely utilized marker-based registration. This technique demands preoperative rigid fixation of fiducial markers—typically radiopaque spheres or ellipsoids coated with reflective material for optical tracking—near the patient, usually affixed via robotic clamping mechanisms. The spatial relationship between these reflective spheres and radiopaque points is predefined. While imaging, the navigation system automatically detects radiopaque markers in the scan, computes their coordinates, and establishes spatial correspondence. The surgeon confirmed successful marker identification to complete registration. Conventional marker-based registration has several critical limitations: (1) The preoperative workflow is cumbersome, requiring robotic arms to clamp and position fiducial arrays in proximity to the patient, with additional intraprocedural intervention necessitating the attachment of calibration targets during imaging acquisition. (2) Crowded operative fields increase positioning complexity and registration failure risk, frequently necessitating repeated registration attempts that prolong the operative

duration. (3) Mandatory rigid fixation of fiducial markers is critical, as any intraoperative displacement introduces registration inaccuracies. (4) Metallic marker components are prone to generating imaging artifacts that compromise diagnostic image quality. (5) Fiducial markers must reside entirely within the imaging volume. In patients with elevated BMI, markers frequently extend beyond this volume, thus precluding successful registration.

In this study, image tracker-based registration is used in this new spinal surgical robot. An optical tracker is attached to the 3D C-arm, typically near the detector panel. This configuration enables the establishment of spatial correspondence between different coordinate systems. Following intraoperative scanning of the surgical site with the 3D C-arm, the acquired volumetric images are automatically transmitted to the robotic system. This facilitates subsequent surgical planning and execution. This registration approach significantly streamlines the workflow and markedly reduces the registration time. This new robotic system employs image tracker-based registration to establish a transformation matrix preoperatively between the C-arm's imaging coordinate system and the spatial coordinates of fiducial markers on a calibration phantom. During intraoperative 3D image acquisition, the spatial coordinates of the fiducial markers on the calibration phantom are calculated in real time by combining the tracked C-arm motion trajectory with the preoperatively established transformation matrix. This enables immediate spatial mapping between the fiducial markers' physical coordinates and their corresponding locations within the acquired volumetric image. This 3D acquisition approach eliminates the need for fiducial marker placement on the patient, requires minimal preoperative preparation, and avoids instrument changes at the robotic arm's end-effector, thereby significantly streamlining the intraoperative workflow. Simultaneous 3D acquisition eliminates the need for robotic arm movement or end-effector fiducial marker deployment. This streamlines equipment positioning and optimizes temporal efficiency during the surgical workflow. A core innovation of this study is the optical tracking registration method, which utilizes C-arm trajectory recognition and a calibration algorithm for rapid, accurate spatial registration. This approach yielded a significant improvement in accuracy for the robot-assisted group over the free-hand group, as shown by the reduced entry point ( $0.98 \pm 0.13$  mm vs.  $5.08 \pm 1.17$  mm,  $p < 0.001$ ) and endpoint deviations ( $1.38 \pm 0.20$  mm vs.  $5.52 \pm 0.87$  mm,  $p < 0.001$ ). Consequently, this high-precision registration contributed to a 96.3% K-wire placement accuracy rate and streamlined the pre-procedural workflow.

This new robotic system incorporates integrated lateral force sensing technology. A high-precision force sensor is mounted on the end-effector flange to continuously monitor

the magnitude and direction of the lateral forces exerted on the surgical instrument. This sensor provides real-time feedback of force vectors to the integrated navigation and positioning system, enabling dynamic intraoperative force control. The software system processes incoming force signals and provides real-time visual feedback of force deviations on the needle navigation interface. This enables continuous intraoperative monitoring of instrument loading, facilitating immediate corrective adjustments during needle placement. The system mitigates the risks of tissue displacement and iatrogenic injury, enhancing procedural safety while ensuring targeting accuracy in robotic-assisted spinal surgery. Another central innovation, high-precision lateral force sensing, was introduced to monitor forces during K-wire insertion, thereby preventing skiving and soft tissue injury. This technology's efficacy is evidenced by the significantly lower NOP in the robot-assisted group versus the freehand group ( $1.11 \pm 0.35$  vs.  $9.85 \pm 3.18$ ,  $p < 0.001$ ), reflecting enhanced operational efficiency and safety. Moreover, the system facilitated the achievement of a significantly larger PAA ( $23.66^\circ \pm 2.45^\circ$  vs.  $10.05^\circ \pm 3.58^\circ$ ,  $p < 0.001$ ), a factor critical for optimizing the biomechanical stability of the pedicle screw. A larger puncture abduction angle is critical for enhancing outcomes in both percutaneous vertebroplasty and pedicle screw placement. Biomechanically, it permits a longer screw path along the pedicle axis, which improves fixation strength, and facilitates optimal, centralized cement diffusion in vertebroplasty, reducing leakage risk. In terms of safety, a more lateral approach inherently widens the margin of safety for the spinal cord and nerve roots by distancing instruments from the medial pedicle wall. This trajectory also preserves the integrity of the superior articular facet joint, thereby minimizing the potential for iatrogenic back pain post-surgery.

As the first clinical evaluation of this new spinal surgical robot, this study provides initial evidence of its targeting accuracy. Our results demonstrate targeting precision comparable to or exceeding values reported in peer-reviewed literature for established robotic spinal systems. This study has several limitations. First, the retrospective study and modest cohort size may limit the generalizability of our findings. Future prospective multicenter trials with expanded samples are warranted to increase the statistical power of these findings. Second, the absence of direct comparative assessment against alternative robotic platforms represents a methodological constraint; future work should incorporate comparative effectiveness analyses. Third, validation in patients with complex spinal deformities remains outstanding. Addressing these gaps constitutes key priorities for subsequent investigations.

In this study, the new spinal surgical robot has reliable K-wire placement accuracy, simplifies intraoperative

procedures, shortens surgical time, reduces trauma, and has great potential and further development value.

**Acknowledgements** Not applicable.

**Author contributions** CHL and ZYC: Designed the study, developed the methodology, and wrote the initial manuscript; DCZ: Performed data analysis, created visualizations; All authors: Critically revised the manuscript for intellectual content, approved the final version, and agreed to be accountable for all aspects of the work.

**Funding** This research was funded by Nanjing Medical University - Nanjing Medical University Second Affiliated Hospital 'Medical-Engineering Integration Innovation Project: YGRH002, Natural Science Foundation of Jiangsu Province China (grant number: BK20230301), Natural Science Foundation of the Jiangsu Higher Education Institutions of China (grant number: 23KJB310010), and Natural Science Foundation of Beijing China (grant number: L246016, L256049).

**Data availability** ALL data can be provided as needed.

## Declarations

**Competing interests** The authors declare no competing interests.

**Consent for publication** All procedures involving human participants conformed to the Declaration of Helsinki. Informed consent was obtained from all individual participants.

**Ethics approval and consent to participate** This study was approved by the Medical Ethics Committee of The Second Affiliated Hospital of Nanjing Medical University (Approval No. 2023-XJ-004-01).

**Open Access** This article is licensed under a Creative Commons Attribution-NonCommercial-NoDerivatives 4.0 International License, which permits any non-commercial use, sharing, distribution and reproduction in any medium or format, as long as you give appropriate credit to the original author(s) and the source, provide a link to the Creative Commons licence, and indicate if you modified the licensed material. You do not have permission under this licence to share adapted material derived from this article or parts of it. The images or other third party material in this article are included in the article's Creative Commons licence, unless indicated otherwise in a credit line to the material. If material is not included in the article's Creative Commons licence and your intended use is not permitted by statutory regulation or exceeds the permitted use, you will need to obtain permission directly from the copyright holder. To view a copy of this licence, visit <http://creativecommons.org/licenses/by-nc-nd/4.0/>.

## References

- Chen AF, Kazarian GS, Jessop GW et al (2018) Robotic technology in orthopaedic surgery. *J Bone Jt Surg* 100:1984–1992. <https://doi.org/10.2106/JBJS.17.01397>
- Fatima N, Massaad E, Hadzipasic M et al (2021) Safety and accuracy of robot-assisted placement of pedicle screws compared to conventional free-hand technique: a systematic review and meta-analysis. *Spine J* 21:181–192. <https://doi.org/10.1016/j.spinee.20.20.09.007>
- Li W, Li G, Chen W et al (2020) The safety and accuracy of robot-assisted pedicle screw internal fixation for spine disease. *Bone Jt Res* 9(10):653–666. <https://doi.org/10.1302/2046-3758.910.BJ.R-2020-0064.R2>
- Li HM, Zhang RJ, Shen CL (2020) Accuracy of pedicle screw placement and clinical outcomes of robot-assisted technique versus conventional freehand technique in spine surgery from nine randomized controlled trials. *Spine* 45(2):E111–E119. <https://doi.org/10.1097/BRS.0000000000003193>
- Lopez IB, Benzakour A, Mavrogenis A et al (2022) Robotics in spine surgery: systematic review of literature. *Int Orthop* 47(2):447–456. <https://doi.org/10.1007/s00264-022-05508-9>
- Farber SH, Pacult MA, Godzik J et al (2021) Robotics in spine surgery: a technical overview and review of key concepts. *Front Surg* 8:578674. <https://doi.org/10.3389/fsurg.2021.578674>
- Sukovich W, Brink-Danan S, Hardenbrook M (2006) Miniature robotic guidance for pedicle screw placement in posterior spinal fusion: early clinical experience with the SpineAssist®. *Int J Med Robot Comput Assist Surg* 2(2):114–122. <https://doi.org/10.1002/rcs.86>
- Barzilay Y, Liebergall M, Fridlander A et al (2006) Miniature robotic guidance for spine surgery — introduction of a novel system and analysis of challenges encountered during the clinical development phase at two spine centres. *Int J Med Robot Comput Assist Surg* 2(2):146–153. <https://doi.org/10.1002/rcs.90>
- Alluri RK, Avrumova F, Sivaganesan A et al (2021) Overview of robotic technology in spine surgery. *HSS Journal: Musculoskeletal J Hosp Special Surg* 17(3):308–316. <https://doi.org/10.1177/15563316211026647>
- Lee NJ, Lombardi JM, Qureshi S et al (2024) Robot-assisted spine surgery: the pearls and pitfalls. *J Am Acad Orthop Surg* 33(2):e81–e92. <https://doi.org/10.5435/JAAOS-D-24-00692>
- Wang MY, Goto T, Tessitore E et al (2017) Introduction. Robotics in neurosurgery. *Neurosurg Focus* 42(5):E1. <https://doi.org/10.3171/2017.2.FOCUS1783>
- Chang J, Yu L, Li Q et al (2022) Development and clinical trial of a new orthopedic surgical robot for positioning and navigation. *J Clin Med* 11:7091. <https://doi.org/10.3390/jcm11237091>
- Lefranc M, Peltier J (2016) Evaluation of the ROSA™ spine robot for minimally invasive surgical procedures. *Expert Rev Med Devices* 13:899–906. <https://doi.org/10.1080/17434440.2016.1236680>
- Jiang B, Karim Ahmed A, Zygourakis CC et al (2018) Pedicle screw accuracy assessment in ExcelsiusGPS® robotic spine surgery: evaluation of deviation from pre-planned trajectory. *Chin Neurosurg J* 4:23. <https://doi.org/10.1186/s41016-018-0131-x>
- Kantelhardt SR, Martinez R, Baerwinkel S et al (2011) Perioperative course and accuracy of screw positioning in conventional, open robotic-guided and percutaneous robotic-guided, pedicle screw placement. *Eur Spine J* 20:860–868. <https://doi.org/10.1007/s00586-011-1729-2>
- Pechlivanis I, Kiriyanthan G, Engelhardt M et al (2009) Percutaneous placement of pedicle screws in the lumbar spine using a bone mounted miniature robotic system: first experiences and accuracy of screw placement. *Spine* 34:392–398. <https://doi.org/10.1097/BRS.0b013e318191ed32>
- Hyun S-J, Kim K-J, Jahng T-A et al (2017) Minimally invasive robotic versus open fluoroscopic-guided spinal instrumented fusions. *Spine* 42:353–358. <https://doi.org/10.1097/BRS.0000000000001778>
- Keric N, Doenitz C, Haj A et al (2017) Evaluation of robot-guided minimally invasive implantation of 2067 pedicle screws. *Neurosurg Focus* 42:E11. <https://doi.org/10.3171/2017.2.FOCUS16552>
- Ringel F, Stürer C, Reinke A et al (2012) Accuracy of robot-assisted placement of lumbar and sacral pedicle screws: a prospective randomized comparison to conventional freehand screw implantation. *Spine* 37:E496–501. <https://doi.org/10.1097/BRS.0b013e31824b7767>



20. Wallace DJ, Vardiman AB, Booher GA et al (2019) Navigated robotic assistance improves pedicle screw accuracy in minimally invasive surgery of the lumbosacral spine: 600 pedicle screws in a single institution. *Int J Med Robot Comput Assist Surg* 16:e2054. <https://doi.org/10.1002/rcs.2054>
21. Zhang JN, Fan Y, Hao DJ (2019) Risk factors for robot-assisted spinal pedicle screw malposition. *Sci Rep* 9:3025. <https://doi.org/10.1038/s41598-019-40057-z>
22. Gautam D, Vivekanandan S, Mazur MD (2025) Robotic spine surgery: systematic review of common error types and best practices. *Oper Neurosurg* 28:295–302. <https://doi.org/10.1227/ons.000000000001293>
23. Vidyadhara S, Iyer RD, Soni A et al (2025) Risk factors of inaccurate screw placement in robotic spine surgeries: why do robots make error and how to avoid them? *J Robot Surg* 19(1):681. <https://doi.org/10.1007/s11701-025-02884-3>
24. Hu X, Ohnmeiss DD, Lieberman IH (2013) Robotic-assisted pedicle screw placement: lessons learned from the first 102 patients. *Eur Spine J* 22(3):661–666. <https://doi.org/10.1007/s00586-012-2499-1>
25. Wang C, Zhang H, Zhang L et al (2021) Accuracy and deviation analysis of robot-assisted spinal implants: A retrospective overview of 105 cases and preliminary comparison to open freehand surgery in lumbar spondylolisthesis. *Int J Med Robot* 17(4):e2273. <https://doi.org/10.1002/rcs.2273>

**Publisher's note** Springer Nature remains neutral with regard to jurisdictional claims in published maps and institutional affiliations.